Available online at www.sciencedirect.com
ScienceDirect
Chinese Journal of Natural Medicines 2020, **18**(4): 243–249
doi: 10.1016/S1875-5364(20)30029-7
Chinese Journal of Natural Medicines

•Special topic•

A new iron(III) chelator of coprogen-type siderophore from the deep-sea-derived fungus *Mycosphaerella* sp. SCSIO z059

HUANG Zhong-Hui[1], LIANG Xiao[1], QI Shu-Hua[1, 2*]

[1] *CAS Key Laboratory of Tropical Marine Bio-resources and Ecology, Guangdong Key Laboratory of Marine Materia Medica, Institution of South China Sea Ecology and Environmental Engineering, South China Sea Institute of Oceanology, Chinese Academy of Sciences, Guangzhou 510301, China;*

[2] *Southern Marine Science and Engineering Guangdong Laboratory, Guangzhou 511458, China*

Available online 20 Apr., 2020

[ABSTRACT] Mycosphazine A (**1**), a new iron(III) chelator of coprogen-type siderophore, and mycosphamide A (**2**), a new cyclic amide benzoate, together with six known aryl amides (**3**−**8**), were isolated from the fermentation broth of the deep-sea-derived fungus *Mycosphaerella* sp. SCSIO z059. Alkaline hydrolysis of **1** afforded a new epimer of dimerum acid, mycosphazine B (**1a**), and a new bi-fusarinine-type siderophore, mycosphazine C (**1b**). The planar structures of the new compounds were elucidated by extensive spectroscopic data analysis. The absolute configurations of amino acid residues in **1a** and **1b** were determined by acid hydrolysis. And the absolute configuration of **2** was established by quantum chemical calculations of the electronic circular dichroism (ECD) spectra. Compound **1** is the first siderophore-Fe(III) chelator incorporating both L-ornithine and D-ornithine unites. Compounds **3**−**8** were reported as natural products for the first time, and the ^{1}H and ^{13}C NMR data of **6** and **8** were assigned for the first time. Compounds **1** and **1a** could greatly promote the biofilm formation of bacterium *Bacillus amyloliquefaciens* with the rate of about 249% and 524% at concentration of 100 μg·mL^{-1}, respectively.

[KEY WORDS] Deep-sea-derived fungus; *Mycosphaerella* sp; Iron(III) chelator; Coprogen-type siderophore; Cyclic amide; Biofilm formation

[CLC Number] R284 **[Document code]** A **[Article ID]** 2095-6975(2020)04-0243-07

Introduction

Iron is an essential element for all microorganisms and an important cofactor required for key cellular, metabolic and biosynthetic processes. Fungi and bacteria are potentially limited by low iron levels in the high-nitrate-low-chlorophyll (HNLC) regions of the world's oceans. To overcome this apparent lack of iron, microorganisms have evolved an elaborate mechanism to acquire Fe(III). Under aerobic growth conditions, fungi, bacteria, and other microorganisms produce siderophores, which are low molecular weight (typically 400−1200 Da), virtually ferric-ion-specific compounds for the solubilization and sequestration of iron(III) [1-3]. Siderophores can be classified into three categories, depending on the ligand moiety for Fe^{3+} coordination: catecholate, hydroxamate/carboxylate, and mixed-type [4]. Besides the sequestration of iron(III), siderophores have been proved to show diverse biological activities, including the ability to function as signaling molecules, regulators of oxidative stress, antibiotics, and enzyme inhibitors to inhibit iron-dependent enzymes by withrawing the metal [4-8]. Interference with siderophore biosynthesis is considered as a therapeutic means to treat microbial infections [7]. Siderophore-antibiotic conjugates have been developed as drug leads with reduced permeability-mediated drug resistance using "Trojan Horse" type mechanisms [9]. Therapeutic iron chelators containing siderophore scaffolds have also been used in the treatments of blood-transfusion requiring diseases [10].

Most fungi, such as the genera *Neurospora*, *Ustilago*, *Rhodotorula*, *Fusarium*, *Aspergillus*, *Penicillium*, have the ability of producing siderophores in response to iron limitation [1]. Fungal siderophores are mainly hydroxamate-type,

[Received on] 20-Dec.-2019
[Research funding] This work was supported by the Guangdong Provincial-level Special Funds for Promoting High-quality Economic Development (No. 2020032), Natural science foundation of Guangdong province (No. 2017A030313235), Key Special Project for Introduced Talents Team of Southern Marine Science and Engineering Guangdong Laboratory (Guangzhou) (No. GML2019-ZD0406), and National Natural Science Foundation of China (No. 81673326). .
[*Corresponding author] E-mail: shuhuaqi@scsio.ac.cn
These authors have no conflict of interest to declare.

which could be classified into three structural groups: ferrichromes, fusarinines (or fusigens), and coprogens [1, 7]. The ferrichromes are cyclic hexapeptide siderophores composed of three N^{δ}-acyl-N^{δ}-hydroxy-L-ornithine, two variable amino acids (alanine, serine, or glycine), and a glycine linked by way of peptide bonds [1, 6-7]. The fusarinines are composed of N^{δ}-hydroxy-N^{δ}-*cis*-anhydromevalonyl-L-ornithine residues [1, 6-7]. The coprogens are a class of diketopiperazines composed of N^{δ}-hydroxyornithine and N^{δ}-anhydromevalonic acid residues [1, 6-7]. To date, all fungal siderophores are derived from L-ornithine, except for neurosporin incorporating D-ornithine [1, 7].

During the course of our search for novel natural products from fungi, we studied on the secondary metabolites of the deep-sea-derived fungus *Mycosphaerella* sp. SCSIO z059 isolated from a deep-sea sediment sample collected at a depth of 1330 m from Okinawa Trough sediment, which resulted in the obtainment of a new iron(III) chelator of coprogen-type siderophore, mycosphazine A (**1**), and a new cyclic amide benzoate, mycosphamide A (**2**), together with six known aryl amides (Fig. 1). Compound **1** was hydrolyzed to offer two new siderophores mycosphazines B and C (**1a** and **1b**) and a known compound N-acetyl-fusarinine (**1c**). Compounds **1**, **1a**−**1c**, and **2** were primarily evaluated for their cytotoxicity, antiviral activity towards HSV-1, toxicity towards brine shrimp, antibacterial, and anti-biofilm activities. Herein we describe the isolation, identification, and bioactivities of these compounds.

Results and Discussion

Mycosphazine A (**1**) was isolated as red amorphous solid. The disturbance of the NMR spectrum by paramagnetic atoms led us suspect that it contained iron, which was supported by HR-ESI-MS displaying a molecular formula of $C_{35}H_{53}N_6O_{13}Fe$ for **1** at *m/z* 822.3114 $[M + H]^+$. Alkaline hydrolysis of **1** gave three compounds (**1a**−**1c**) and $Fe(OH)_3$ sediment [11]. The structures of **1a**−**1c** were determined by extensive spectroscopic data analysis as following.

Compound **1a** was obtained as colorless powder. The molecular formula was determined to be $C_{22}H_{36}N_4O_8$ by HR-ESI-MS at *m/z* 485.2612 $[M + H]^+$. The ^{13}C NMR spectrum of **1a** exhibited 11 carbon resonances including one methyl, five methylenes, one methine, one tri-substituented double bond, and two acyl groups, which indicated that **1a** had a completely symmetrical system. The ^1H and ^{13}C NMR data of **1a** (Table 1) showed great similarity to that of dimerum acid which was the dimer of N^{δ}-hydroxy-N^{δ}-*trance*-anhydromevalonyl-L-ornithine (*trance*-fusarinine) forming a diketopiperazine ring [12-15]. The ^1H-^1H COSY spectrum (Fig. 2) showed sequential correlations of NH-2/H-2/H-3/H-4/H-5, NH-2′/H-2′/H-3′/H-4′/H-5′, H-9/H-10/OH-10, and H-9′/H-10′/OH-10′, respectively, which indicated the presence of two symmetrical -NHCHCH$_2$CH$_2$CH$_2$- and -CH$_2$CH$_2$OH fragments. The HMBC spectrum (Fig. 2) showed correlations of H-2/H-3 with C-1, H-5 with C-6, H-7 with C-6 and C-8, H-9 with C-7 and C-8, and H-11 with C-7, C-8 and C-9. The above data suggested that **1a** had the same planar structure as dimerumic acid. The NOESY spectrum showing correlation between H-7 and H-9 suggested the *E* geometry of the double bond ($\Delta^{7,8}$) [15], which was supported by the great similarity of ^1H and ^{13}C NMR data of the N^{δ}-anhydromevalonyl moieties (C6−C11) in **1a** and dimerumic acid [15]. The absolute configurations of amino acid residues were further determined by acid hydrolysis. Dried acid hydrolysates of **1a** were analyzed by HPLC with a MCI GEL CRS10W column and compared with authentic standards. Although the retention time (t_R) of authentic standard D-Orn was close to that of L-Orn, it was clear to confirm that **1a** contained one L-Orn and one D-Orn residues (data not shown). Actually, we also tried to determine the absolute configurations of amino acid residues by Marfey's method and HPLC analysis. The retention time of the FDAA derivate of D-Orn was also close to that of the FDAA derivate of L-Orn in HPLC chromatogram with an ODS column. The analysis results of hydrolysates of **1a** in the two methods were consistent. Thus, the structure of **1a** was elucidated as shown. It was an epimer of dimerum acid, and named mycosphazine B.

Compound **1b** had a molecular formula of $C_{22}H_{38}N_4O_9$ as inferred from its HR-ESI-MS at *m/z* 503.2732 $[M + H]^+$. The ^1H and ^{13}C NMR data of **1b** (Table 1) showed similarity

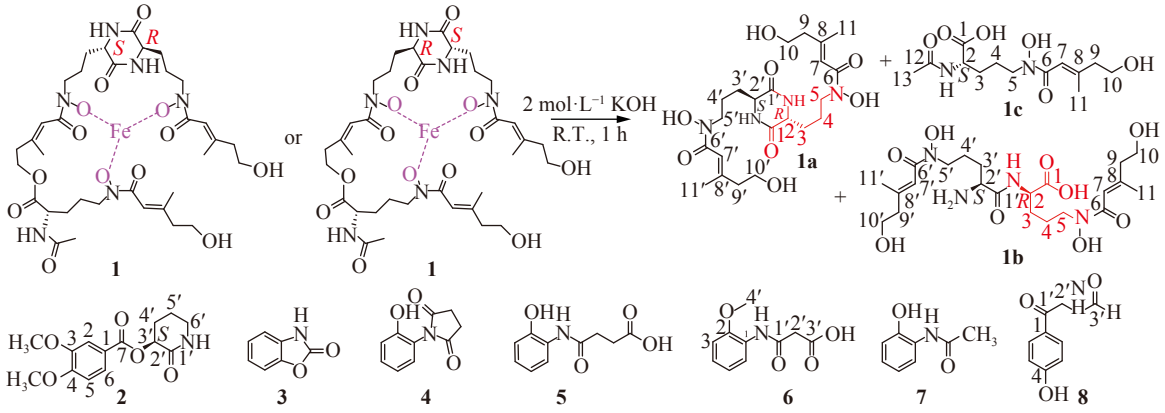

Fig. 1 Structures of compounds 1−8 and 1a−1c

Table 1 ^{1}H NMR (500 MHz) and ^{13}C NMR (125 MHz) data for compounds 1a–1c (DMSO-d_6)

1a			1b			1c		
No.	δ_H (*J* in Hz)	δ_C, type	No.	δ_H (*J* in Hz)	δ_C, type	No.	δ_H (*J* in Hz)	δ_C, type
1/1′		167.9, C	1		172.9, C	1		173.6, C
2/2′	3.84, m	53.7, CH	1′		168.5, C	2	4.14, m	51.7, CH
3/3′	1.66, m	29.8, CH_2	2	4.26, m	51.8, CH	3	1.52, m; 1.66, m	28.3, CH_2
4/4′	1.55, m	21.6, CH_2	2′	3.83, br s	52.0, CH	4	1.56, m	23.2, CH_2
5/5′	3.48, t (7.0)	46.8, CH_2	3	1.57, m; 1.69, m	28.4, CH_2	5	3.50, t (6.5)	46.6, CH_2
6/6′		166.5, C	3′	1.71, m	28.8, CH_2	6		166.6, C
7/7′	6.21, br s	116.1, CH	4	1.57, m	22.0, CH_2	7	6.22, br s	116.1, CH
8/8′		151.0, C	4′	1.57, m	22.9, CH_2	8		151.1, C
9/9′	2.23, t (6.6)	43.8, CH_2	5/5′	3.51, t (5.9)	46.6, CH_2	9	2.24, t (6.6)	43.8, CH_2
10/10′	3.53, t (6.7)	59.2, CH_2	6/6′		166.7, C	10	3.53, t (6.7)	59.2, CH_2
11/11′	2.02, br s	18.2, CH_3	7/7′	6.23, br s	116.1, CH	11	2.02, br s	18.2, CH_3
2/2′-NH	8.15, d (1.3)		8/8′		151.2, C	12		169.3, C
5/5′ N-OH	9.63, br s		9/9′	2.24, t (6.7)	43.8, CH_2	13	1.84, s	22.3, CH_3
10/10′-OH	4.52, t (6.5)		10/10′	3.54, t (6.5)	59.2, CH_2	2-NH	8.11, d (7.7)	
			11/11′	2.02, s; 2.03, s	18.3, CH_3	5 N-OH	9.63, br s	
			2-NH	8.71, d (7.9)		COOH	12.50, br s	
			2′-NH_2	8.13, br s				
			5/5′ N-OH	9.66, s; 9.69, s				
			COOH	12.87, br s				
			10/10′-OH	4.56, br s				

to that of **1a**, and the ^{13}C NMR spectrum of **1b** showing 15 carbon resonances indicated that **1b** had a partially symmetric system. Diagnostic 2D NMR correlations (Fig. 2) revealed assembly of the planar structure as shown, inclusive of *E* configurations of $\Delta^{7,8}$ and $\Delta^{7',8'}$. The absolute configurations of amino acid residues were also determined by acid hydrolysis. HPLC analysis of hydrolysates of **1b** with a MCI GEL CRS10W column confirmed the incorporation of L-Orn and D-Orn units (Data not shown), permitting the identification of **1b** as shown, namely mycosphazine C. We speculated that **1b** derived from the amidation of one molecule of N^{δ}-hydroxy-N^{δ}-*trance*-anhydromevalonyl-L-ornithine and one molecule of N^{δ}-hydroxy-N^{δ}-*trance*-anhydromevalonyl-D-ornithine forming a linear dipeptide.

Compound **1c** was identified to be the known compound *N*-acetyl-fusarinine by spectroscopic analysis and comparison with literature data [12]. The ^{1}H and ^{13}C NMR data of **1c** (Tables 1−2) were assigned for the first time. HPLC analysis for hydrolysates of **1c** with a MCI GEL CRS10W column further confirmed that **1c** contained one L-Orn residue (Data not shown).

Based on the structures of hydrolysates **1a**−**1c** and the molecular formula of $C_{35}H_{53}N_6O_{13}Fe$, two possible structures were proposed for **1** as shown in Fig. 1. Owing to lack of more experimental evidence, the linkage between the moieties of **1a** and **1c** in compound **1** could not be determined. It was the first siderophore-Fe(III) chelator incorporating both L-ornithine and D-ornithine unites.

Compound **2** was acquired as yellowish oil, and its molecular formula was found to be $C_{14}H_{17}NO_5$ based on the HR-ESI-MS at *m/z* 302.1004 $[M + Na]^+$ and NMR data (Table 2). The ^{13}C and DEPT NMR spectra revealed 14 carbon signals corresponding to two carbonyl carbons, three aromatic non-hydrogen carbons, three aromatic methines, one oxygenated methine, three methylenes, and two methoxy groups. The ^{1}H NMR spectrum of **2** showed signals at δ_H 7.08 (1H, br s, H-2), 7.00 (1H, d, *J* = 8.0 Hz, H-5), 7.14 (1H, d, *J* = 8.0 Hz, H-6), indicating that **2** contained a trisubstituted aromatic system. The HMBC spectrum showing correlations from 3-OMe (δ_H 3.78) to C-2/C-3/C-4, from 4-OMe (δ_H 3.80) to C-3/C-4/C-5, and from H-2/H-6 to C-7, and the ^{1}H-^{1}H COSY spectrum showing correlation between H-5 and H-6, suggested the presence of a 3,4-dimethoxy-1-benzoate fragment. In addition, the ^{1}H-^{1}H COSY spectrum showing sequential correlations of H-3′/H-4′/H-5′/H-6′, and the HMBC spectrum showing correlations from H-3′/H-4′/H-6′ to C-2′ (Fig. 2), sugges-

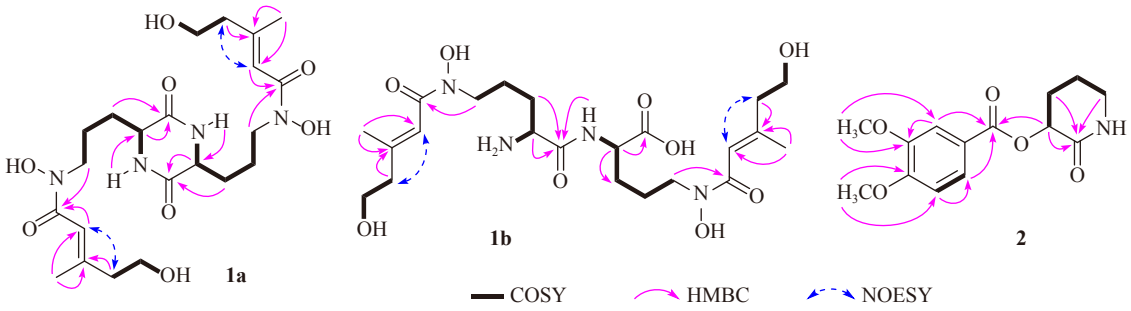

Fig. 2 Key 2D NMR correlations for compounds 1a, 1b and 2

ted the presence of a 3′-hydroxyl-2′-piperidinone fragment. The HMBC correlation from H-3′ to C-7 suggested the 3,4-dimethoxy-1-benzoate fragment connected to C-3′ of the 3′-hydroxyl-2′-piperidinone moiety through an ester bond.

The absolute configuration of C-3′ in **2** was further determined by quantum chemical calculations of ECD spectra at the PBE1PBE/6-311G(d) level in Gaussian 09. The experimental CD spectrum of **2** showed negative cotton effects at the wave lengths of 203 and 252 nm, which was similar to that of 3′*S*-**2**, and opposite to that of 3′*R*-**2** (Fig. 3). Thus, **2** was inferred to have 3′*S* configuration. This was also supported by comparing the specific rotation values of **2** ($[\alpha]_D^{25}$ −36.6 (*c* 0.10, MeOH)) and the synthetic compound 12 ($[\alpha]_D^{25}$ −19.0 (*c* 0.67, MeOH)) in literature [16].

The other compounds were identified to be 2-benzoxazolinone (**3**) [17], *N*-(2-hydroxyphenyl)-succinimide (**4**) [18], 4-[(2-hydroxyphenyl)amino]-4-oxobutanoic acid (**5**) [19], 3-(methoxyphenylamino)-3-oxopropanoic acid (**6**) [20], 2-acetylamino-phenol (**7**) [21], and *N*-[2-(4-hydroxyphenyl)-2-oxoethyl]-formamide (**8**) [22] by spectroscopic analysis and comparisons with literature data. Compounds **3**–**8** were reported as synthetic products in literatures. The ^{1}H and ^{13}C NMR data of **6** and **8** (Table 2) were assigned for the first time.

Compounds **1**, **1a**–**1c**, and **2** were evaluated for their cytotoxicity against Vero cell line by MTT method, and for their antiviral activity towards HSV-1 by cytopathic effect (CPE) assay. Unfortunately, all the compounds didn't show obvious cytotoxicity with IC_{50} > 100 mg·mL^{-1}, and didn't have antiviral activity at concentration of 100 μg·mL^{-1}.

Furthermore, compounds **1**–**8** and **1a**–**1c** were also primarily evaluated for their toxicity towards brine shrimp, antibacterial and anti-biofilm activities towards marine bac-

Table 2 ^{1}H NMR (500 MHz) and ^{13}C NMR (125 MHz) data for compounds 2, 6, and 8 (DMSO-d_6)

No.	2		6		8	
	δ_H (*J* in Hz)	δ_C, type	δ_H (*J* in Hz)	δ_C, type	δ_H (*J* in Hz)	δ_C, type
1		128.3, C		127.2, C		125.2, C
2	7.08, br s	111.0, CH		149.0, C	7.83, d (8.7)	130.4, CH
3		148.1, C	7.04, dd (8.1, 1.6)	111.1, CH	6.80, d (8.7)	115.7, CH
4		150.3, C	7.07, m	124.2, CH		164.1, C
5	7.00, d (8.0)	110.8, CH	6.91, m	120.2, CH	6.80, d (8.7)	115.7, CH
6	7.14, d (8.0)	120.4, CH	8.05, dd (7.9, 1.0)	121.0, CH	7.83, d (8.7)	130.4, CH
7		167.8, C				
1′				164.7, C		192.3, C
2′		173.4, C	3.49, s	43.3, CH_2	4.55, d (5.6)	43.8, CH_2
3′	4.37, dd (8.3, 4.7)	59.1, CH		169.9, C	8.15, s	161.4, CH
4′	1.88, m; 2.25, m	28.9, CH_2	3.84, s	55.7, CH_3		
5′	1.84, m	25.1, CH_2				
6′	3.57, m	49.7, CH_2				
3-OMe	3.78, m	55.4, CH_3				
4-OMe	3.80, m	55.5, CH_3				
NH			9.56, s		8.29, s	

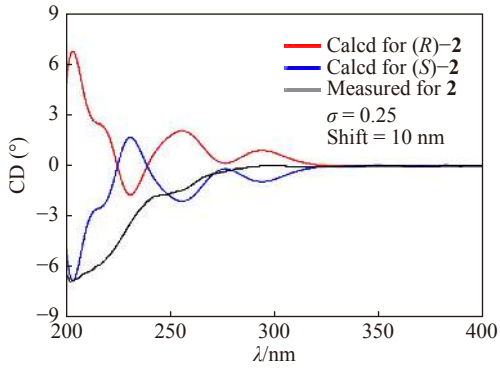

Fig. 3 Comparison between calculated and measured ECD spectra of 2 in MeOH

terium *Bacillus amyloliquefaciens* SCSGAB0082 and common pathogenic bacteria *Staphylococcus aureus*, *Pseudomonas aeruginosa*, *B. subtilis*, and *Escherichia coli* at concentration of 100 μg·mL^{-1}. The results showed that **5**, **8**, and **9** had weak toxicity towards brine shrimp naupalii with lethality of about 40%−60%, while the other compounds had no obvious toxicity. In addition, all the compounds didn't have obvious antibacterial activity against the growth of the five tested bacteria, and only **5** and **6** exhibited anti-biofilm activity against the biofilm formation of *B. amyloliquefaciens* and *E. coli* with inhibiting rate of about 50%−60%. On the contrary, compared with the blank control (LBS medium), **1** and **1a** could greatly promote the biofilm formation of *B. amyloliquefaciens* with the rate of about 249% and 524% at concentration of 100 μg·mL^{-1} , respectively. In the test, penicillin G sodium salt, gentamicin sulfate salt, and streptomycin sulfate were used as the positive controls.

The indicator bacterium *B. amyloliquefaciens* SCSGAB0082 isolated from the South China Sea gorgonian in our laboratory, could produce antimicrobial surfactins and iturins, showing moderate or strong antibacterial activity against Gram-positive bacteria including *B. subtilis*, *S. aureus* and *Micrococcus luteus* [23]. Our preliminary study on the effects of different metal cations on pellicle formation of *B. amyloliquefaciens* showed that low amount of Fe^{2+} and Fe^{3+} exhibited positive effects on pellicle formation, but overabundant Fe^{2+} and Fe^{3+} led to the decrease of pellicle biomass. More details about the mechanism are under study. In this study, we speculated that **1** and **1a** affected the concentrations of Fe^{3+} in pellicle cells, leading to promoting the pellicle formation of *B. amyloliquefaciens*.

Experimental

General experimental procedures

Optical rotations were recorded on an Anton Paar MCP 500 polarimeter. UV and IR spectra were measured using Shimadzu UV-2600 UV-vis spectrophotometer and Shimadzu IR Affinity-1 Fourier transform infrared spectrophotometer, respectively. NMR spectroscopic data were acquired with a Bruker AV-500 MHz NMR spectrometer with TMS as an internal standard. HR-ESI-MS spectra were performed on a Bruker MaXis quadrupole-time-of-flight mass spectrometer. ECD spectrum was measured with a Chirascan circular dichroism spectrometer (Applied Photophysics Ltd). Semi-preparative reversed-phase HPLC was performed on a Shimadzu LC-20A preparative liquid chromatography system with an YMC-Pack ODS column (250 mm × 20 mm I.d., 5 μm). Column chromatography (CC) was performed on silica gel (200−300 mesh, Qingdao Marine Chemical Factory, Qingdao, China), Sephadex LH-20 (GE Healthcare), and ODS (40−63 μm, YMC, Japan).

Fungal materials

The fungus *Mycosphaerella* sp. SCSIO z059 (Genbank accession number KX258811) was isolated from a deep-sea sediment sample collected at a depth of 1330 m from Okinawa Trough (27°48.47'N, 126°54.32'E). It was identified as *Mycosphaerella* sp. 99% according to ITS rDNA sequence data. The sequence of this strain showed a 99% identity with *Mycosphaerella* sp. AA-2012 (GenBank accession number JQ732904). The strain was deposited in the RNAM Center, South China Sea Institute of Oceanology, Chinese Academy of Sciences.

Fermentation and extraction

Spores of the fungal strain were inoculated into 300 mL sterilized liquid medium (glucose 1%, mannitol 2%, maltose 2%, monosodium glutamate 1%, yeast extract 0.3%, corn steep liquor 0.05%, KH_2PO_4 0.05%, $MgSO_4·7H_2O$ 0.03%, dissolved in sea water, pH 6.5) in Erlenmeyer flasks (1000 mL) followed by static fermentation at 26 °C for 30 days. After filtration of the mycelium, the culture broth (50 L) was mixed with XAD-16 resin (20 g·L^{-1}) and stirred at low speed for three hours to absorb the organic products. The resin was washed with distilled water to remove medium composition then eluted with ethanol. The ethanol solvent was removed under reduce pressure to obtain a brown residue (16.3 g). The mycelia were extracted with acetone for three times. The acetone extract was evaporated under vacuum to afford an aqueous solution, and then extracted with ethyl acetate to give a crude gum (21.7 g).

Isolation and purification

The combined extract was subjected to silica gel column (200−300 mesh) chromatography eluting with $CHCl_3$/MeOH (*V*/*V*, 100 : 0–50 : 50) to give six fractions (Fr.1–Fr.6). Fr.2 was further fractionated on a silica gel column (200−300 mesh) eluting with $CHCl_3$/acetone (*V*/*V*, 100 : 0−50 : 50) to give five sub-fractions (Fr. 2-1–Fr. 2-5). Fr. 2-1 was chromatographed on an ODS column (2.6 cm × 31 cm, MPLC) with a step gradient of MeOH/H_2O/TFA (*V*/*V*/*V* 10 : 90 : 0.03−100 : 0 : 0.03) to afford four sub-fractions (Fr. 2-1-1–Fr. 2-1-4). Fr. 2-1-2 was submitted to a Sephadex LH-20 column ($CHCl_3$/MeOH, *V*/*V* 1 : 1) followed by preparative HPLC eluting with CH_3CN/H_2O (*V*/*V*, 10 : 90) to give **7** (t_R = 28.9 min, 29.6 mg). Fr. 2-1-4 were isolated by preparative HPLC (CH_3OH/H_2O, *V*/*V*, 32 : 68) to yield **3** (t_R = 22.0 min, 5.8 mg), **4** (t_R = 27.5 min, 2.3 mg), **5** (t_R = 25.2 min, 3.0 mg), respectively. Fr.2-2 was applied to an ODS column using

CH_3OH/H_2O (*V/V* 20 : 80−100 : 0) as eluent to provide three sub-fractions (Fr. 2-2-1–Fr. 2-2-3). Compound **6** (t_R = 31.0 min, 16.9 mg) was isolated from Fr. 2-2-2 by purification of Sephadex LH-20 ($CHCl_3$/MeOH, *V/V*, 1 : 1) and preparative HPLC (CH_3OH/H_2O, *V/V*, 30 : 70). Fr. 2-3 was submitted to an ODS column using MeOH/H_2O/TFA (*V/V/V* 10 : 90 : 0.03−100 : 0 : 0.03) as mobile phase to get two sub-fractions (Fr. 2-3-1–Fr. 2-3-2). Fr. 2-3-1 was separated by preparative TLC (CH_2Cl_2/MeOH, *V/V*, 9 : 1), then subjected to a Sephadex LH-20 column (MeOH) to obtain **8** (4.2 mg). Fr. 2-3-2 was applied to column chromatography on Sephadex LH-20, followed by preparative HPLC eluting with CH_3OH/H_2O (*V/V* 35 : 65) to afford **2** (t_R = 28.4 min, 12.0 mg). Fr. 3 was separated by MPLC with an ODS column, eluting with MeOH/H_2O (*V/V* 15 : 85−100 : 0) to give three sub-fractions (Fr. 3-1−Fr. 3-3). Fr. 3-2 was chromatographed over a Sephadex LH-20 column to get **1** (53.3 mg).

*Alkaline hydrolysis of compound **1***

A solution of compound **1** (25 mg) in MeOH (2.5 mL) was stirred with 2 mol·L^{-1} KOH (4 mL) at room temperature for 1 h. The mixture was centrifuged to separate $Fe(OH)_3$ and the supernatant. Then the supernatant was neutralized with dilute hydrochloric acid and separated with HPLC (CH_3CN/H_2O/TFA, 11 : 89 : 0.03) to yielded compounds **1a** (6.7 mg), **1b** (4.3 mg), **1c** (7.5 mg).

Characteristics of compounds

*Mycosphazine A (**1**)*

Red amorphous solid; $[\alpha]_D^{25}$ −30.3 (*c* 0.10, MeOH/H_2O 30 : 70); UV (MeOH) λ_{max} (log ε) 206 (4.36), 247 (4.03), 433 (3.21) nm; IR (film) ν_{max} 3255, 1732, 1658, 1537, 1454, 1377, 1327 cm^{-1}; HR-ESI-MS *m/z* 822.3095 $[M + H]^+$, *m/z* 844.2926 $[M + Na]^+$.

*Mycosphazine B (**1a**)*

Colorless powder; $[\alpha]_D^{25}$ 0 (*c* 0.10, MeOH); UV (MeOH) λ_{max} (log ε) 218 (4.19) nm; IR (film) ν_{max} 1674, 1645, 1562, 1462, 1446, 1425, 1342, 1311 cm^{-1}; HR-ESI-MS *m/z* 507.2433 $[M + Na]^+$ (Calcd. for $C_{22}H_{36}N_4O_8Na$, 507.2425).

*Mycosphazine C (**1b**)*

Colorless powder; $[\alpha]_D^{25}$ +1.3 (*c* 0.10, MeOH); UV (MeOH) λ_{max} (log ε) 218 (3.60) nm; IR (film) ν_{max} 1674, 1598, 1444, 1427, 1381, 1201, 1184, 1138, 1022 cm^{-1}; HR-ESI-MS *m/z* 525.2527 $[M + Na]^+$ (Calcd. for $C_{22}H_{38}N_4O_9Na$, 507.2531).

*N-acetyl-fusarinine (**1c**)*

Yellowish oil; $[\alpha]_D^{25}$ +9.5 (*c* 0.10, MeOH); HR-ESI-MS *m/z* 325.1376 $[M + Na]^+$ (Calcd. for $C_{13}H_{22}N_2O_6Na$, 325.1370).

*Mycosphaloid A (**2**)*

Yellowish oil; $[\alpha]_D^{25}$ −36.6 (*c* 0.10, MeOH); UV (MeOH) λ_{max} (log ε) 206 (4.28), 252 (3.75), 282 (3.48) nm; IR (film) ν_{max} 1716, 1602, 1573, 1517, 1456, 1429, 1334, 1261, 1236, 1178 cm^{-1}; HR-ESI-MS *m/z* 302.1004 $[M + Na]^+$ (Calcd. for $C_{14}H_{17}NO_5Na$, 302.0999).

*Determination of absolute configurations of **1a−1c***

Compounds **1a**−**1c** (0.5 mg each) dissolved in HCl (6 mol·L^{-1} , 1 mL) were collected in a sealed glass bottle and kept at 115 °C for 15 h, respectively. After cooling, the hydrolysate was evaporated and dissolved in 400 μL H_2O. Aliquots (5 μL) of each analyte were subjected to HPLC analysis (MCI GEL CRS10W column, 3 μm, 50 mm × 4.6 mm, 0.2 mL·min^{-1}, 0.1 mmol·L^{-1} $CuSO_4$ aq. solution as mobile phase) at an absorbance of 340 nm, with comparison to authentic standards D/L-Orn (0.125 mg·mL^{-1}).

Antibacterial and anti-biofilm bioassay

Compounds **1**−**8** and **1a**−**1c** were tested for their antibacterial and anti-biofilm activities towards five bacteria including marine bacterium *Bacillus amyloliquefaciens* SCSGAB0082 and common pathogenic bacteria *Staphylococcus aureus*, *Pseudomonas aeruginosa*, *B. subtilis*, and *Escherichia coli* in 96-well plates [24]. All of the tested compounds were dissolved in dimethyl sulfoxide (DMSO). Compounds **1**−**8** and **1a**−**1c** were primarily tested at concentration of 100 μg·mL^{-1}, and the positive controls including penicillin G sodium salt, gentamicin sulfate salt, and streptomycin sulfate were tested at concentration of 50 μg·mL^{-1}.

References

[1] Holinsworth B, Martin JD. Siderophore production by marine-derived fungi [J]. *BioMetals*, 2009, **22**: 625–632.

[2] Springer SD, Butler A. Microbial ligand coordination: consideration of biological significance [J]. *Coord Chem Rev*, 2016, **306**: 628–635.

[3] Gadd GM. Microbial influence on metal mobility and application for bioremediation [J]. *Geoderma*, 2004, **122**(2−4): 109–119.

[4] Li K, Chen WH, Bruner SD. Microbial siderophore-based iron assimilation and therapeutic applications [J]. *BioMetals*, 2016, **29**: 377–388.

[5] Timothy C, Johnstone EMN. Beyond iron: non-classical biological functions of bacterial siderophores [J]. *Dalton Trans*, 2015, **44**(14): 6320–6339.

[6] Renshaw JC, Robson GD, Trinci APJ, *et al*. Fungal siderophores: structures, functions and applications [J]. *Mycol Res*, 2002, **106**(10): 1123–1142.

[7] Braun V, Winkelmann G. Microbial iron transport structure and function of siderophores [J]. *Pro Clini Biochem Medi*, 1987, **5**: 67–99.

[8] Chi Z, Wang XX, Ma ZC, *et al*. The unique role of siderophore in marine-derived *Aureobasidium pullulans* HN6.2 [J]. *BioMetals*, 2012, **25**: 219–230.

[9] Go'rska A, Sloderbach A, Marszałł MP. Siderophore-drug complexes: potential medicinal applications of the "Trojan horse" strategy [J]. *Trends Pharmacol Sci*, 2014, **35**(9): 442–449.

[10] Olivieri NF, Brittenham GM, Matsui D, *et al*. Iron-chelation therapy with oral deferiprone in patients with thalassemia major [J]. *N Engl J Med*, 1995, **332**(14): 918–922.

[11] Assante G, Camarda L, Locci R, *et al*. Isolation and structure of red pigments from *Aspergillus ñavus* and related species, grown on a differential medium [J]. *J Agr Food Chem*, 1981, **29**: 785–787.

[12] Harrington GJ, Neilands JB. Isolation and characterization of dimerum acid from *Verticillium dahlia* [J]. *J Plant Nutr*, 1982, **5**: 675–682.

[13] Hördt W, Römheld V, Winkelmann G. Fusarinines and dimerum acid, mono- and dihydroxamate siderophores from *Penicillium chrysogenum*, improve iron utilization by strategy I and

strategy II plants [J]. *BioMetals*, 2000, **13**: 37–46.
[14] Krasnoff SB, Keresztes I, Donzelli BGG, *et al*. Metachelins, mannosylated and N-oxidized coprogen-type siderophores from *Metarhizium robertsii* [J]. *J Nat Prod*, 2014, **77**(7): 1685–1692.
[15] Kalansuriya P, Quezada M, Esposito BP, *et al*. Talarazines A-E: noncytotoxic iron(III) chelators from an Australian mud dauber wasp-associated fungus, *Talaromyces* sp. (CMB-W045) [J]. *J Nat Prod*, 2017, **80**(3): 609–615.
[16] Mai HDT, Thanh GV, Tran VH, *et al*. Synthesis of febrifuginol analogues and evaluation of their biological activities [J]. *Tetrahedron Lett*, 2014, **55**(52): 7226–7228.
[17] Liu P, Wang Z, Hu X. Highly efficient synthesis of ureas and carbamates from amides by iodosylbenzene-induced Hofmann rearrangement [J]. *Eur J Org Chem*, 2012, **10**: 1994–2000.
[18] Caulfield MJ, Looney MG, Pittard RA, *et al*. Studies on polyimides. Part 1: synthesis of model compounds and their reaction with hexamethylenetetramine [J]. *Polymer*, 1998, **39**(25): 6541–6548.
[19] Trujillo-Ferrara J, Santillan R, Beltran HI, *et al*. ^{1}H and ^{13}C NMR spectra for a series of arylmaleamic acids, arylmaleimides, arylsuccinamic acids and arylsuccinimides [J]. *Magn Reson Chem*, 1999, **37**(9): 682–686.
[20] Saavedra OM, Claridge SW, Zhan L, *et al*. Inhibitors of VEGF receptor and HGF receptor signaling: US, 2007/0004675 [P]. 2007.
[21] Moreno-Corral R, Hopfl H, Machi-Lara L, *et al*. Synthesis, structural characterization and metal inclusion properties of 18-, 20- and 22-membered oxaazacyclophanes and oxaazacalix [4]arene analogues: macrocyclic amine and schiff base receptors with variable NxOy donor sets [J]. *Eur J Org Chem*, 2011, **11**: 2148–2162.
[22] Hagedorn I, Eholzer U, Etling H. Isonitrile, V.$^{+}$ Darstellung von *α.β*-ungesättigten isonitrilen, *β*-keto- und *β*-chlo-isonitrilen. Synthese des Xanthocillin-dimethyläthers [J]. *Eur J Inorg Chem*, 1965, **98**: 193–201.
[23] Peng J, Zhang X, Xu X, *et al*. Diversity and chemical defense role of culturable non-actinobacterial bacteria isolated from the South China Sea gorgonians [J]. *J Microbiol Biotechnol*, 2013, **23**: 437–443.
[24] Wang J, Nong XH, Zhang XY, *et al*. Screening of anti-biofilm compounds from marine-derived fungi and the effects of secalonic acid D on *Staphylococcus aureus* biofilm [J]. *J Microbiol Biotechnol*, 2017, **27**(6): 1078–1089.

Cite this article as: HUANG Zhong-Hui, LIANG Xiao, QI Shu-Hua. A new iron(III) chelator of coprogen-type siderophore from the deep-sea-derived fungus *Mycosphaerella* sp. SCSIO z059 [J]. *Chin J Nat Med*, 2020, **18**(4): 243-249.